Energy 278 (2023) 127880

Contents lists available at ScienceDirect

Energy

journal homepage: www.elsevier.com/locate/energy

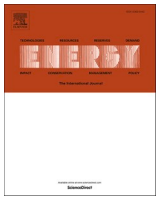

Ammonia from solid fuels: A cost-effective route to energy security with negative CO_2 emissions

Carlos Arnaiz del Pozo [a], Schalk Cloete [b,*], Ángel Jiménez Álvaro [a]

[a] Universidad Politécnica de Madrid, Spain
[b] SINTEF Industry, Norway

ARTICLE INFO

Handling Editor: Krzysztof (K.J.) Ptasinski

Keywords:
Ammonia
CO_2 capture
Gasification
Techno-economic assessment
Energy carrier
Energy security

ABSTRACT

This study investigates a potential solution to the global challenge of secure, affordable, and low-carbon energy supply: ammonia production from local coal and biomass resources with CO_2 capture for negative emissions. Two innovative configurations; an E-gas gasifier with membrane-assisted water-gas shift and an air-blown MHI gasifier design, are compared with an oxygen-blown GE gasifier benchmark. Under the baseline cost assumptions of 2.5 €/GJ for coal, 6.1 €/GJ for biomass, and a CO_2 tax of 100 €/ton, the GE configuration reached a levelized cost of ammonia (LCOA) of 391.5 €/ton, while the E-gas and MHI concepts showed 59.0 (−15.1%) and 18.6 (4.8%) €/ton lower and higher costs, respectively. Subsequent benchmarking against alternative ammonia supply pathways showed that the energy security offered by the E-gas configuration comes at a premium of around 40% over ammonia imported at cost from natural gas exporting regions, which will be cheaper than liquified natural gas if the CO_2 price exceeds 60.9 €/ton. Since prices of imported energy are generally well above the cost of production, the carbon-negative energy security offered by the proposed plants can be economically attractive to importers with rising CO_2 taxes. Thus, policy support for establishing local ammonia value chains can be recommended.

1. Introduction

Curtailment of greenhouse gas (GHG) emissions from the energy and agricultural sectors is of central importance in climate change mitigation [1]. To extend global decarbonization efforts beyond the electricity sector, adoption of carbon free energy carriers such as hydrogen has become a mid to long-term objective in the energy transition [2]. However, hydrogen presents techno-economic challenges with regards to transportation and storage [3], prompting increasing research and development efforts on circumventing these drawbacks by introducing an additional conversion step to other chemical compounds that are easier to handle.

Ammonia (NH_3) presents relevant advantages as an energy carrier since it is a liquid at −33.4 °C and 1 bar, making it easy to store and transport over long distances. For example, an International Energy Agency (IEA) analysis [4] identified ammonia as the most cost-effective pathway for intercontinental hydrogen trade. Since ammonia synthesis is well-known and optimized for several decades [5], the key requirement for its adoption as a prominent future energy carrier is a low-cost, low-carbon hydrogen feed. Such a feed stream can originate from hydrocarbon fuels with CO_2 capture (blue hydrogen) or from electrolysis driven by renewable electricity (green hydrogen).

A previous study by the authors [6] found blue ammonia costs of 385.9 €/ton and 332.1 €/ton for conventional and advanced technologies, respectively. The green route based on projected mid-century technology costs proved considerably more expensive (e.g., 540.6 €/ton using the high-quality solar resource in Southern Spain [6]). However, natural gas supply security for importing regions such as Europe is a considerable drawback associated with the cost-effective blue ammonia routes investigated in the aforementioned study, although this concern would be partially mitigated in a flexible and diversified international liquified ammonia market based on shipping rather than pipelines. To avoid energy security concerns, ammonia production from cheap and locally available coal resources [7] offers a compelling alternative. Despite its higher carbon intensity, capital costs and more complex process layout, increased supply security presents a worthwhile trade-off in world regions such as China, responsible of 95% of global coal-based NH_3 production [8].

For perspective, NH_3 from coal origin and natural gas steam methane reforming (SMR) represent 22% and 72% of the global total [9], respectively. Ghavam et al. [10] carried out a review of life cycle

* Corresponding author. Flow Technology Group, SINTEF Industry, S.P. Andersens vei 15B, 7031, Trondheim, Norway.
E-mail address: schalk.cloete@sintef.no (S. Cloete).

https://doi.org/10.1016/j.energy.2023.127880
Received 24 September 2022; Received in revised form 2 May 2023; Accepted 17 May 2023
Available online 22 May 2023

Acronyms

ACF	Annualized cash flows
ASME	American Society of Mechanical Engineers
ASU	Air Separation Unit
BEC	Bare erected cost.
CAPE	Computer-aided process engineering
CCS	Carbon capture & storage
CFB	Circulating Fluidized Bed.
CGE	Cold gas efficiency
EPC	Engineering, procurement and construction
EoS	Equation of state
FOM	Fixed operating & maintenance costs
GE	General Electric
GHG	Greenhouse gas
GSR	Gas switching reforming
HGCU	Hot gas clean up.
HTS	High temperature shift
KBR	Kellogg Brown & Root
LAC	Linde Ammonia Concept
LCOA	Levelized cost of ammonia
LCOP	Levelized cost of product
LHV	Lower heating value
LPG	Liquefied petroleum gases
LNG	Liquefied natural gas
MA-ATR	Membrane assisted autothermal reforming
MAWGS	Membrane assisted water gas shift reactor
MDEA	Methyl di-ethanol amine
MHI	Mitsubishi Heavy Industries
NET	Negative emissions technology
NPV	Net present value
OC	Owners costs
PC	Process contingency
PSA	Pressure swing adsorption
PT	Project contingency
RE	Renewable energy
RES	Renewable energy sources
SEA	Standardized economic assessment
SMR	Steam methane reforming
TOC	Total overnight cost
TRL	Technology readiness level
T&S	Transport & storage
tpd	Tons per day
VOM	Variable operating & maintenance cost
WGS	Water gas shift

List of Symbols

η	Thermal efficiency
φ	Capacity factor
i	Discount rate
n	Plant lifetime
t	Year
C_i	Annualized capital or operation cost
C_{CO_2}	Specific capture
E_{CO_2}	Specific emissions
P_{NH_3}	Yearly NH_3 production
SC	Specific consumption (GJ/ton)
$\dot{m}$	Mass flow (kg/s)
$\dot{W}$	Power (kW)

assessment (LCA) studies of sustainable NH_3 production underlining the importance of consistent system boundary definition for appropriate benchmarking, while revealing that NH_3 from SMR resulted in higher GHG emissions albeit lower water consumption than that produced from water electrolysis. Arora et al. [11] indicate that the Global Warming Potential (GWP) on a life cycle basis of coal derived ammonia amounts to 4.2 kg of $CO_{2,eq}$ per kg of NH_3 relative to 2.81 kg/kg for natural gas. However, the GWP of ammonia production can potentially fall by 3.0 kg/kg when biomass is used as gasification feedstock instead of coal. Indeed, the adoption of a tax on CO_2 emissions motivates both integration of carbon capture and storage (CCS) technologies and partial coal-to-biomass fuel switching through co-gasification, thereby potentially attaining net negative CO_2 emissions. Furthermore, commercial NH_3 process configurations are well-suited for CCS since the added plant scope is limited to a CO_2 compressor, although associated transport and storage infrastructure must be available.

Such a co-gasification strategy offers advantages beyond climate change mitigation: 1) The detrimental effect on efficiency due to lower energy density of biomass is reduced, 2) constraints regarding the limited availability of sustainable biomass resources are mitigated, and 3) more aggressive biogenic molten ash that may limit refractory lifetime of entrained flow gasifiers can be sufficiently diluted, allowing high-temperature gasification that avoids undesired tar formation [12]. In pursuit of these benefits, successful co-gasification of 30%w biomass blended with coal in an Integrated Gasification Combined Cycle (IGCC) plant have been reported [13]. Larger fractions of up to 70% on an energy basis have been attempted with torrefied biomass by Thattai et al. [14], remarking that increasing biomass fractions in existing gasification plants are possible without major modifications, although this may pose a challenge in terms of resource availability for the large-scale production processes intended in this study.

Gasification technology selection is another important consideration. Habgood et al. [15] highlight the lack of economic viability of NH_3 production based on moving bed gasification, but underline the low cost of downstream urea production and excess CO_2 sequestering relative to capture from electricity generation. On the other hand, circulating fluidized bed (CFB) gasifiers present low carbon conversion and higher methane contents [16]. Xu et al. [17] provide an overview of recent developments on coal conversion to fuels underlining that dry-feed entrained flow gasification technology is the preferred choice for large scale applications. However, despite the lower thermal efficiency and higher oxygen consumption of slurry-fed systems, higher operating pressures can be reached compared to dry feeding [12], which can be advantageous for the design and performance of downstream units.

Following the gasification step, subsequent process units for NH_3 production involve the cooling and treating of the gaseous product [18]. Due to the prevalence of carbon atoms in the syngas, extensive water gas shift (WGS) is required to generate the H_2 reactant, which involves considerable steam consumption as well as further reduction of overall efficiency due to the exothermicity of the reaction. H_2 separated from the purified shifted syngas is then supplied with N_2 from the air separation unit (ASU) and fed to the NH_3 synthesis loop. Two avenues for process design are explored from the basis of a standard synthesis loop intended for large production capacities [19] coupled to the H_2 plant presented in an IEAGHG study [20], with the goal of maximizing the thermal conversion of fuel to H_2 while delivering an inert-free syngas stream to the loop. The first approach consists of transposition of proven and mature technological components employed in existing NH_3 processes or IGCC plants. Thus, the re-arrangement and integration of these units gives place to an innovative and cost competitive process with relatively low associated risk. The second approach combines several technological step-outs and process intensification with the objective of attaining a drastic reduction in levelized cost of product. These elements

involve advanced gasification designs [21], high temperature syngas treating [22], membrane reactors to simultaneously carry out shift and separation [23,24] and advanced heat integration strategies. A techno-economic assessment of this advanced process configuration will reveal the gains that may be expected from maturing the pre-commercial units involved to inform subsequent research and development efforts.

Thus, the present study bridges a significant literature gap with respect to process design and techno-economic benchmarking of advanced coal/biomass-to-NH_3 configurations for secure, affordable, and carbon-negative fuel supply in a future net-zero world. In particular, the innovative design using pre-commercial technology shows substantial cost-reduction potential (~15% below the reference technology) with potential for further gains (~26% below the reference) if district heating can be implemented. The district heating integration is a realistic possibility because the novel concept generates no flue gas (and thus no local air pollution). Aside from outlining a pathway to substantial economic and environmental gains, the study offers further novelty with a broader benchmarking study against relevant alternatives, including NH_3 from natural gas and renewables and the direct use of liquified natural gas (LNG). The resulting comparison provides valuable perspective to policymakers in energy importing regions by quantifying the cost of energy security via local production.

In the following section, a succinct overview of the configurations developed with their key features is presented. Subsequently, the methodological approach to the modelling, plant performance evaluation and economic analysis assumptions is thoroughly discussed. The energy, environmental and economic results, with capital and operational cost breakdown and pertinent sensitivity studies of the levelized cost of ammonia (LCOA) to key assumptions, are provided. Following the economic assessment, a broader benchmarking study against NH_3 from other sources as well as LNG provides additional perspective. Finally, the main outcomes of the study are summarized, and the core conclusions are drawn.

1.1. Technology overview

Fig. 1 presents an outline of the NH_3 plants developed, which have been labelled according to the gasification technology employed in each one of them.

- **GE**: A slurry-fed entrained flow gasifier generates syngas which is routed to a sour water gas shift (WGS) unit. After selective CO_2 and H_2S removal with Selexol, a pressure swing adsorption (PSA) unit delivers high purity H_2 to the synthesis loop. Stoichiometric N_2 is provided by the ASU, while the off-gas is used for steam production in a boiler.
- **MHI**: Syngas is generated by means of an air-blown dry-fed entrained flow gasifier with O_2 enriched air from a cryogenic unit. After the WGS unit, H_2S and CO_2 are sequentially removed with methyldiethanolamine (MDEA) absorption. Subsequently, a cryogenic purifier adjusts the syngas module to the stoichiometric requirements of the synthesis reaction, while generating a fuel stream for power generation.
- **E-gas**: A two-stage slurry-fed entrained flow gasifier with chemical quench is used to produce syngas with a high thermal efficiency. A hot gas clean-up (HGCU) unit removes sulphur species and other contaminants prior to a membrane assisted water gas shift reactor (MAWGS) reactor, where nitrogen from the ASU and process steam are used to sweep the membranes to attain a stoichiometric feed to the synthesis loop and to maximize H_2 recovery. The retentate stream is combusted with pure O_2 to provide heat for steam generation and slurry feed vaporization.

GE and MHI plants utilize technology components which do not require major development for their commercialization and are commonly integrated in ammonia synthesis processes [5] or H_2/power generation in Integrated Gasification Combined Cycle (IGCC) plants [20]. On the other hand, the E-gas concept necessitates several technological breakthroughs for successful deployment at large scale. Namely, the two-stage gasification system enhanced through heat integration to reap further efficiency gains must be demonstrated [21], while de-risking of interconnected fluidized bed reactor technology at high pressure for syngas desulphurization and contaminant removal are mandatory to prevent efficiency losses due to cooling (for low temperature treating) or alternatively avoid deleterious effects on the membrane reactor performance downstream when fed with untreated syngas [25]. Furthermore, it must be demonstrated that the high selectivity and permeability of the H_2 perm-selective membranes [26] used in the MAWGS reactor can be maintained over long operating periods under the high pressures assumed in this process. Finally, oxy-combustion of the retentate product assisted with a metallic oxygen carrier is assumed to attain full conversion of the stream.

2. Methodology

In this section a detailed overview of the NH_3 plants from solid fuels is presented. Such plants are designed to reach production capacities of 3000 tpd, through a synthesis loop described in earlier work [6], based on the work developed by Flórez-Orrego et al. [19], employing an iron-based catalyst with a kinetic law derived from Dyson and Simon [27]. The Redlich-Kwong Soave equation of state (EoS) was selected in the synthesis loop for an adequate estimation of vapour-liquid equilibrium. A Douglas Premium coal [28] blended with 30%w woody biomass [29] was assumed as input to the plants. The ultimate and proximate analysis of these feedstocks are tabulated in the Supplementary Material file. Stationary plant simulations were developed in Unisim Design R481, employing the Peng Robinson EoS for property estimation of main process streams according to thermodynamic guidelines [30], while ASME tables were used for steam and water. On the other hand, property estimation of the MAWGS reactor was carried out with an in-house thermodynamic database (Patitug). A schematic of the methodology and modelling tools to carry out the techno-economic assessment of the different concepts is shown in Fig. 2.

2.1. Plant description

The plants illustrated in Fig. 1, labelled according to the gasification technology employed, are thoroughly discussed below. For simplicity, only the connections between the main process blocks are shown without illustrating the heat integration schemes, but full details are available in complete process diagrams and stream summaries presented in the Supplementary Material, alongside the modelling assumptions of the plant units.

2.1.1. GE

Referring to Fig. 1A, the GE gasification of a 65%w. solids slurry (stream 1) is carried out at 80 bar with an oxidant stream (stream 2) delivered by a pumped liquid oxygen air separation unit, at a temperature of 1350 °C, to reach a cold gas efficiency (CGE) of 73.0% and a carbon conversion of 99.5%. High pressure operation is selected based on the maximum achievable for slurry-fed gasifiers reported by Higman [12] to minimize syngas product compression requirements while presenting a high CO_2 partial pressure for absorption. Stream 3 must be cooled from 1350 °C to 400 °C before entering the WGS unit, and this is accomplished in two steps: 1) a radiant syngas cooler generates high pressure (HP) steam while cooling the syngas to around 900 °C before 2) a water quench achieves further cooling to 400 °C, while simultaneously providing the correct amount of steam to drive the WGS reactions. The hot water effluent from the syngas quench is used to preheat the slurry to 200 °C. Subsequently, CO is converted to H_2 in the WGS unit, modelled with two-stage adiabatic reactors to reach equilibrium conversions.

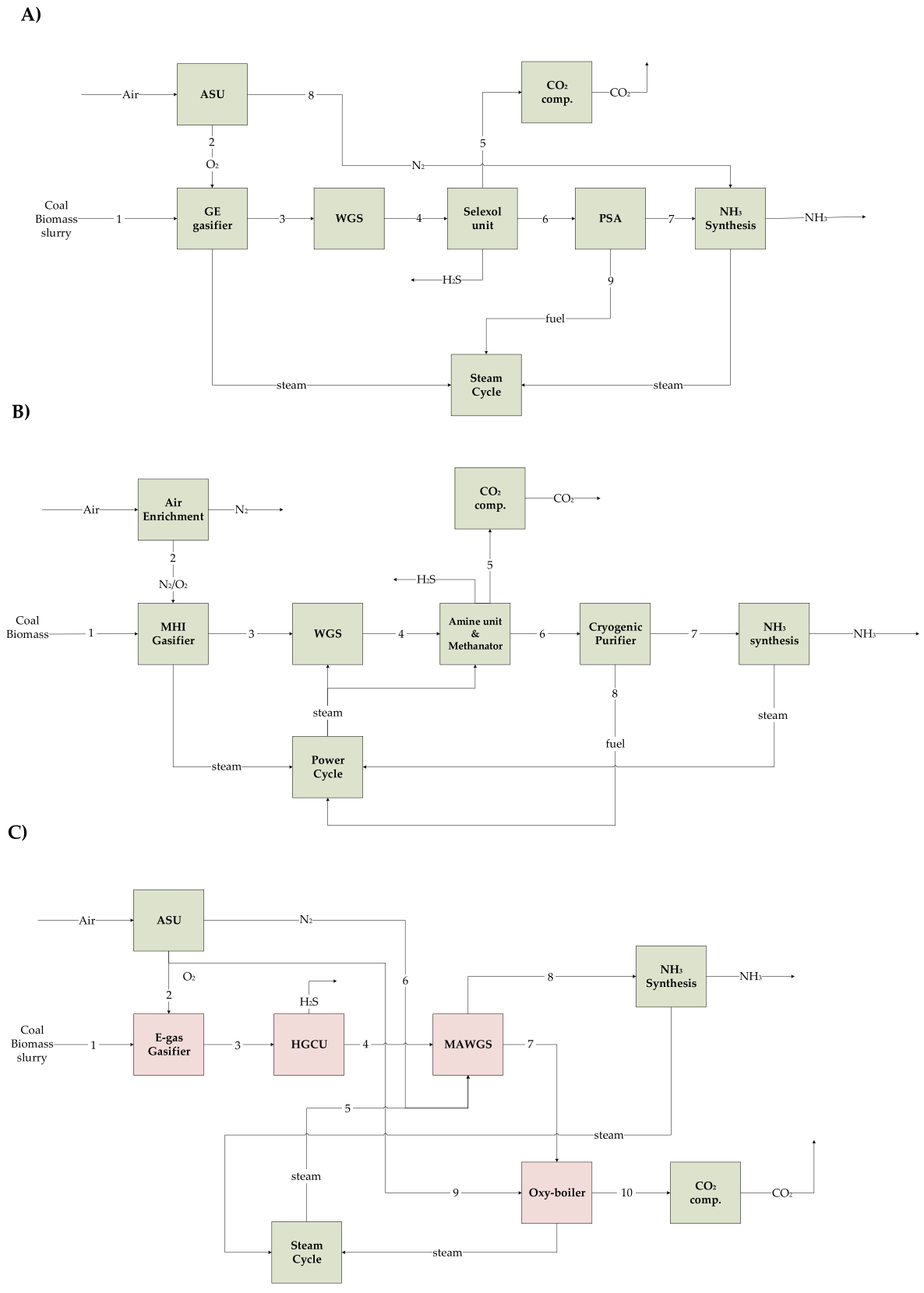

Fig. 1. Block flow diagram of the A) GE, B) MHI and C) E-gas NH_3 plants from solid fuels.

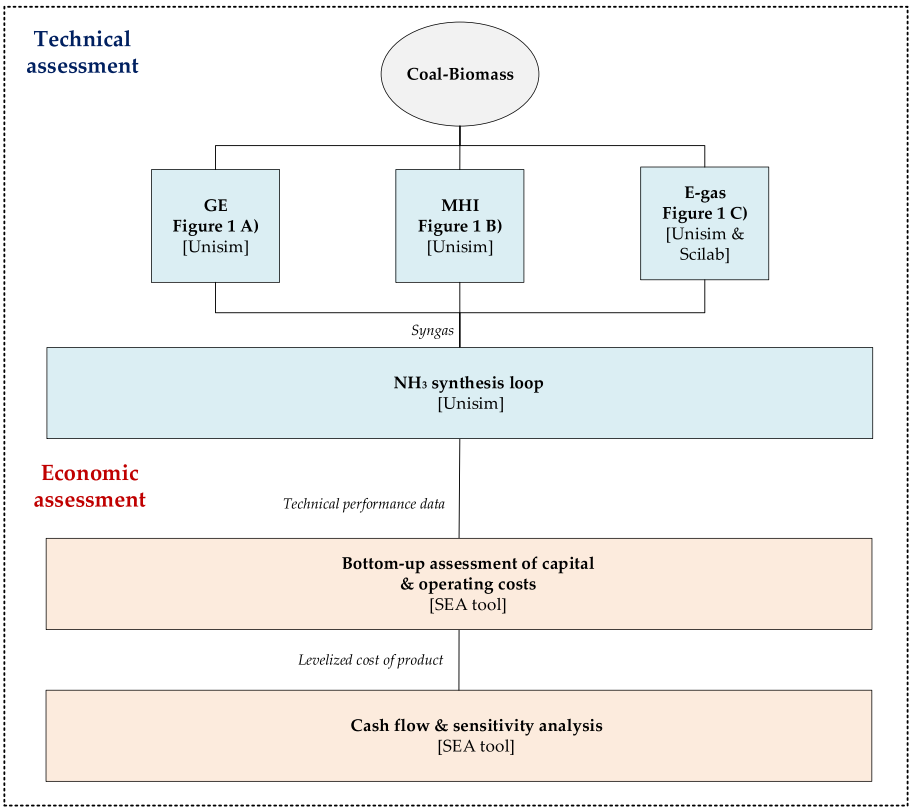

Fig. 2. Methodology and modelling tools employed in the techno-economic assessment.

After heat recovery via HP water economization and water knock-out from stream 4, a dual Selexol unit operated at 25 °C selectively removes around 90% of the CO_2 (stream 5) and all the H_2S present in the syngas. The unit is modelled with Henry coefficients derived from Kapetaki et al. [31]. CO_2 is compressed in a five-stage intercooled compressor and pumped to 150 bar. A significant advantage of employing a physical solvent for CO_2 removal is that regeneration is carried out through pressure let down, and only a small amount of thermal duty in the form of LP steam is required in the H_2S stripper reboiler. The CO_2-lean effluent stream (stream 6) is routed to a PSA unit modelled according to Nazir et al. [32] achieving approximately a 90% recovery of H_2. This high purity hydrogen stream (stream 7) is mixed with a stoichiometric amount of N_2 from the ASU (stream 8), which is compressed to the H_2 pressure of around 65 bar, and then further boosted to 150 bar after mixing, before being fed to the synthesis loop. The low-pressure PSA off-gas (stream 9) is used as fuel in a boiler to produce steam and hot water, which is adequately integrated with the different heat sources of the process (syngas cooling, WGS and NH_3 synthesis heat of reaction).

2.1.2. MHI

The MHI NH_3 plant depicted in Fig. 1B employs an air blown entrained flow gasifier operating at 30 bar where the coal-biomass blend (stream 1) is fed through lock hoppers using CO_2 as a transport gas. The gasifier consists of a combustor stage, where approximately 70% of the feed is reacted with O_2 enriched air at 38.3%mol. purity (stream 2) from a cryogenic unit while the remaining 30% is fed to the reductor stage, attaining a CGE of 80.2%. Operating pressure is limited due to dry feed loading and a downstream purification unit, which results in additional capital costs for syngas compression prior to the synthesis loop. The gasifier was modelled according to Giuffrida et al. [33,34], reaching a combustion temperature of 1900 °C and a temperature drop of 700 °C in the reductor. The gasification model was tuned to reach a similar methane heating value contribution in the syngas product as the values reported by MHI [35]. This is an important factor in the design and operation of the gasifier, which is influenced by the solid fuel properties, given that methane and other higher molecular weight hydrocarbons present in the syngas cannot be ultimately converted to NH_3, thereby decreasing efficiency.

The cryogenic unit delivering the oxidant stream has a similar design to the N_2 production process discussed in Arnaiz and Cloete [6] for NH_3 production from natural gas in the Linde Ammonia Concept (LAC). The advantages of O_2 enrichment are twofold: a higher CGE is achieved while the N_2 concentration is reduced relative to gasification with air, therefore reducing the excess that must be removed in subsequent syngas processing.

The syngas product at 1200 °C (stream 3) has a $(H_2+CO)/N_2$ ratio of 1.72, which is below the synthesis reaction stoichiometry (note that CO is converted to H_2 downstream to a large extent). It is cooled down to 350 °C by first evaporating and subsequently superheating HP steam, thus avoiding undesirable metal dusting at high temperatures [36]. The syngas effluent is then mixed with intermediate pressure (IP) steam to reach a steam to carbon ratio of 1.9, prior to a sour WGS unit. Between and after two adiabatic WGS reactors, heat is recovered from stream 4 to produce IP steam which is mixed with the syngas feed and HP hot water for the syngas effluent coolers and ammonia loop. After cool-down to ambient temperature and water knock out (stream 4), H_2S in the syngas is removed through amine absorption modelled in a simplified way as a component splitter, assuming CO_2 entrainment and reboiler duty consumption based on Giuffrida et al. [34]. Downstream, the bulk of the CO_2 is removed (stream 5) with a capture efficiency of 99.8% in an MDEA unit [37]. LP steam at 1.8 bar from a backpressure turbine is delivered to the amine reboiler for solvent regeneration. It can be mentioned that the chilled ammonia process for post-combustion CO_2 capture has been proposed in an IGCC plant with MHI gasification [38], which could present integration benefits for NH_3 production since a chilling system is already required for product liquefaction, NH_3 is available on-site and NH_3 slip would not be critical as an initial

condensation step in the downstream synthesis unit is present. However, high removal rates under the present process conditions would be required to be competitive with the commercial amine system. A methanation unit downstream the absorber eliminates remaining molecules of CO and CO_2 which would otherwise poison the NH_3 reactor catalyst. This constitutes a relevant efficiency loss as H_2 is consumed in the exothermic reaction with the resulting low-grade heat being rejected. Furthermore, the CH_4 product is an undesirable inert species which accumulates in the synthesis loop, as it lowers the partial pressure of the reactants and therefore conversion per pass, requiring larger purge fractions with resulting reactant losses, unless it is removed beforehand. Therefore, the syngas product (stream 6) is routed to a cryogenic purification unit, where the H_2/N_2 ratio is adjusted to the ammonia synthesis reaction stoichiometry while eliminating all impurities except for a small Ar fraction in the product syngas (stream 7), originating from the enriched air oxidant stream.

Additionally, a low pressure N_2-rich fuel (stream 8) with all CH_4 and some H_2 representing approximately 12% of the syngas inlet heating value is delivered from the cryogenic unit after compression to an aeroderivative gas turbine combustor, which drives the main air compressor and the booster of the cryogenic unit producing enriched air fed to the gasifier. A direct drive configuration enables a more efficient fuel conversion with decreased equipment count, and it will accelerate start-up with natural gas relative to the alternative of boilers and a steam cycle powering electrically driven compressors. However, the different operating points of the gas turbine (GT) with syngas and natural gas may present operational challenges. This configuration is employed in the Kellogg Brown & Root (KBR) plant to deliver compressed air to an autothermal reformer, as presented in earlier work [6].The GT exhaust is used to heat HP water for the NH_3 loop heat recovery exchangers. The GT was calibrated based on vendor data from Badeer [39] to estimate a reasonable performance but, given the large volumetric flow and low energy density of the fuel, it is expected that the GT will operate with a decreased air intake and substantially higher power output relative to nominal values. Suitable modifications to the GT components are assumed and calibrated efficiencies and design pressure ratio are preserved in the model. HP superheated steam from the gasifier and ammonia loop is expanded in a steam turbine, which does not present a low-pressure stage and large condenser operating at vacuum pressure due to the large extraction of IP steam for mixing with WGS syngas feed and additionally, LP steam amine reboiler demand, thus enabling attractive capital cost reductions. The small excess of LP steam is cooled down and recycled to the heat recovery network.

2.1.3. E-gas

The E-gas NH_3 plant showed in Fig. 1C produces syngas from a coal-biomass blend (stream 1) by means of a two-stage slurry fed gasifier [40]. The 1st stage operates at 1350 °C and 80 bar by direct gasification of approximately 79% of the feed, with an oxidant stream delivered by an ASU (stream 2). The remaining fraction is fed to the second stage where sensible heat in the syngas from the first stage drives the endothermic gasification of the remaining 21% of the fuel. This chemical quench converts thermal energy into chemical potential energy, thereby enhancing CGE while achieving partial syngas cooling to 950 °C. To minimize capital costs of the gasifier island, a partial water quench cools stream 3 to approximately 450 °C while adding the steam required for the downstream WGS step. Before WGS, stream 3 is routed to a hot gas clean up unit (HGCU) for desulphurization and contaminant removal consisting of two interconnected fluidized beds (adsorber & regenerator) using ZnO to remove sulphur species, which was modelled according to Giuffrida et al. [22]. N_2 from the ASU is used to dilute the O_2 content of the regenerator inlet stream to 2%mol, where the solid sorbent is re-oxidized and then recycled to the adsorber. A low O_2 concentration is required to mitigate undesired reactions that poison the adsorbent.

The contaminant-free syngas (stream 4) is then routed to the MAWGS reactor [41], modelled with a membrane permeation model based on Fernandez et al. [42] and WGS kinetics of a high temperature catalyst [43]. Although the H_2-perm selective membranes used in the MAWGS reactor are not yet widely available, start-up companies and research institutes are beginning to bring this technology to market.[1] The MAWGS reactor is preceded by a conventional high temperature WGS reactor for bulk CO conversion, with heat recovery exchangers generating IP steam. Maximum operating temperature in the MAWGS reactor was limited to 500 °C to prevent membrane deterioration by suitably cooling the syngas feed to the reactor [24]. High pressure operation is desirable to maximize H_2 permeation across the membrane surface and thus CO conversion by shifting the equilibrium reaction to the products side. The reactor is operated counter-currently, with IP steam (stream 5) and stoichiometric N_2 sweep (stream 6) on the permeate side at low temperature to further enhance conversion by quenching the exothermic reaction, achieving a CO conversion around 91% and a hydrogen recovery of close to 96%. The addition of steam in the sweep reduces the hydrogen partial pressure on the permeate side, enabling a high permeate pressure of 20 bar to minimize compression requirements of the syngas fed to the NH_3 loop (stream 8).

The retentate outlet (stream 7) is reacted with O_2 (stream 9) from the ASU in an oxy-combustion boiler for steam superheating and water economization, which is supplied to the synthesis loop, while a fraction of the heat in stream 10 is used for slurry vaporization to further enhance the CGE of the gasifier. Given the low concentration of combustible species in the MAWGS retentate outlet, this fuel heating value is retrieved by supporting the reaction with an oxygen carrier [44], to ensure full conversion. The benefits of this arrangement include complete CO_2 capture in stream 10, preservation of the stream pressure to minimize CO_2 compression duty and a simpler heat integration for slurry pre-heating and vaporization.

2.2. Energy and environmental performance indicators

Energy efficiency in Eq. (1) is defined as the ratio between the lower heating value of the NH_3 product and the solid fuel heat input. On the other hand, the equivalent efficiency in Eq. (2) takes into account the net electricity exports of the plant ($\dot{W}_{net}$ is negative for electricity imports) with a heat to power conversion factor of 45.5% corresponding to a reference advanced ultra-supercritical coal plant [28]. Finally, the electric efficiency is expressed according to Eq. (3). as the ratio between the net power generation and the primary energy input.

$$\eta_{NH_3} = \frac{\dot{m}_{NH_3} LHV_{NH_3}}{\dot{m}_{bio} LHV_{bio} + \dot{m}_{coal} LHV_{coal}} \tag{1}$$

$$\eta_{NH_3,eq} = \frac{\dot{m}_{NH_3} LHV_{NH_3}}{\dot{m}_{bio} LHV_{bio} + \dot{m}_{coal} LHV_{coal} - \frac{\dot{W}_{net}}{\eta_{el}}} \tag{2}$$

$$\eta_{El.} = \frac{\dot{W}_{net}}{\dot{m}_{bio} LHV_{bio} + \dot{m}_{coal} LHV_{coal}} \tag{3}$$

Alternatively, the specific energy consumption defined in Eq. (4) gives account of the fuel heat input per mass unit of product, while the equivalent specific energy consumption in Eq. (5). Incorporates the relative contribution of power generation or demand of the plant.

$$SC = \frac{\dot{m}_{bio} LHV_{bio} + \dot{m}_{coal} LHV_{coal}}{\dot{m}_{NH_3}} \tag{4}$$

[1] E.g., https://www.hydrogen-mem-tech.com/technology, https://www.h2site.eu/en/and https://www.tecnalia.com/en/technologies/membrane-technology-and-process-intensification.

$$SC_{eq} = \frac{\dot{m}_{bio} LHV_{bio} + \dot{m}_{coal} LHV_{coal} - \frac{\dot{W}_{net}}{\eta_{el}}}{\dot{m}_{NH_3}} \quad (5)$$

In terms of environmental performance, Eq. (6). shows the CO_2 emissions per mass unit of NH_3, E_{CO_2}. Under the assumption that biomass emissions are carbon-neutral, only emissions from coal origin are accounted for in the calculation, while captured biogenic emissions are subtracted. Negative emissions can be achieved if emissions from coal origin are lower than captured emissions from biomass origin, thus requiring a sufficiently high CO_2 capture ratio and biomass blend ratio. Similarly, the specific capture rate C_{CO_2} reflects the amount of CO_2 that must be stored per unit of product.

$$E_{CO_2} = \frac{\dot{m}^{coal}_{CO_2,emit} - \dot{m}^{bio}_{CO_2,capt}}{\dot{m}_{NH_3}} \quad (6)$$

$$C_{CO_2} = \frac{\dot{m}^{coal}_{CO_2,capt} + \dot{m}^{bio}_{CO_2,capt}}{\dot{m}_{NH_3}} \quad (7)$$

2.3. Economic assumptions

The economic assessment of the NH_3 plants from solid fuels was carried out with the Standardized Economic Assessment Tool developed by the authors [45]. A user guide is available for download [46]. The economic evaluation consists of a bare erected cost (BEC) estimation of the different plant units through Turton [47] or capacity-cost correlations obtained from literature [28,48]. The total overnight cost (TOC), calculated in 2020 Euros (€) for plants located in Western Europe, is determined from the BEC estimation according to the cost factors detailed in Table 1, where the economic assumptions for fixed (FOM) and variable (VOM) operating & maintenance costs are also presented.

Targeting a mid-century energy system with a large role for low-carbon fuels like ammonia, all process configurations are assessed as commercially mature plants with similar project contingencies, engineering and owner's costs, and capacity factors. However, due to the technological uncertainties of several units of the E-gas configuration, process contingencies (PC) of 30% for the MAWGS and HGCU units and 10% for the heat recovery network with oxy-boiler combustion and slurry vaporization were added to prevent overoptimistic cost estimations for these pre-commercial units. Due to the lack of availability in literature for entrained flow, dry-fed air-blown gasifier cost estimations at the scale of the present plants, the MHI unit cost was estimated assuming a capacity-cost correlation for a Shell gasifier derived from a DOE report [48], due to the technological similarities. Nevertheless, a dedicated sensitivity study for the cost assumptions of these units in the three cases is presented later.

Table 1
Economic assumptions.

Capital estimation methodology		
Bare erected cost (BEC)		SEA Tool Estimate
Engineering procurement and construction (EPC)		10% BEC
Process contingency (PC)		0–30% BEC
Project contingency (PT)		20% (BEC + EPC + PC)
Owner's costs (OC)		15% (BEC + EPC + PT + PC)
Total overnight costs (TOC)		BEC + EPC + PC + PT + OC
Operating & maintenance costs		
Fixed		
Maintenance	2.5	%TOC
Insurance	1	%TOC
Labour	60000	€/y-p
Operators	120	persons
Variable		
Coal	2.5	€/GJ
Biomass	100	€/ton
Electricity	60	€/MWh
NH_3 catalyst	20	€/kg
WGS catalyst	16100	$/ton
CO_2 tax	100	€/ton
CO_2 transport & storage	20	€/ton
Process water	6	€/ton
Cooling water make-up	0.35	€/ton
Ash disposal	9.73	€/ton
Absorbent make-up	5000	€/ton
NiO oxygen carrier	15	$/kg
Cash flow analysis assumptions		
1st year capacity factor	65	%
Remaining years	85	%
Discount rate	8	%
Construction period	4	years
Plant Lifetime	25	years

The cash flow analysis is performed to determine the levelized cost of product (LCOP), defined as the selling price at which the net present value (NPV) in Eq. (8) of the plant adds up to zero for a given capacity factor (φ) and maximum yearly NH_3 production (P_{NH_3}). The NPV is the summation of discounted cash flows (Eq. (9)) across the plant lifetime.

$$NPV = \sum_{t=0}^{n} \frac{ACF_t}{(1+i)^t} \quad (8)$$

$$ACF_t = \varphi \cdot \left(LCOP \cdot P_{NH_3} - C_{VOM}\right) - C_{Capital} - C_{FOM} \quad (9)$$

In order to present a wide perspective of the economic potential of the configurations developed in this work, several sensitivity studies of the LCOP to key economic assumptions are presented. Namely, the influence of coal & biomass prices, gasifier capital cost, CO_2 tax, CO_2 transport & storage costs, discount rate and plant capacity factor are consistently evaluated.

3. Results

Results are provided in three subsections. First, the energy and environmental performance of each plant is presented and then the economic results are shown, with corresponding sensitivity analysis to key economic assumptions. Subsequently, the cost of product on an energy basis for the configurations proposed in this study is benchmarked against LNG and blue NH_3 from natural gas to convey a holistic perspective of the potential of NH_3 from local solid fuels as source of climate-friendly and cost-effective energy security.

3.1. Energy & environmental results

The energy breakdown for the different configurations is provided in Table 2. The GE configuration reveals the lowest thermal efficiency resulting from the low CGE of the gasifier (73.0%), shift conversion losses and combustion of the fuel heating value of the PSA off-gas, leading the highest primary energy input requirements. The two-stage gasification of the E-gas process enables an improved fuel efficiency by 11.3 %-points relative to the GE plant. Accounting for power imports, this represents an equivalent specific energy consumption reduction of 5.2 GJ/ton (−14.2%). This large increase in performance is achieved through enhanced CGE efficiency (87.3%) and lower thermal losses in syngas processing steps of the advanced concept. On the other hand, MHI thermal performance gains are limited to 3.0 %-points relative to GE, corresponding to 2.2 GJ/ton (−6.3%) lower equivalent consumption. The substantially larger CGE of the air-blown two-stage gasifier (80.2%) is offset by thermal losses in the methanation reactor and cryogenic purification unit.

When comparing the power breakdown for the E-gas plant to that of the GE benchmark, the decreased O_2 consumption caused by the high CGE results in comparatively lower ASU power demand while the pressurized combustion of the MAWGS retentate minimizes CO_2 compression duty, yielding an overall auxiliary consumption which represents 10.9% of the heat input. In comparison, electricity consumption amounts to 12.9 and 14.9% of the primary energy input for the GE and MHI cases, respectively. In the latter case, the reduced

Table 2
Energy and environmental results of the NH_3.

Item/Plant		GE	MHI	E-gas
Energy balance				
Coal LHV	MWth	991.9	935.5	813.3
Biomass LHV	MWth	277.7	261.9	227.7
NH_3 LHV	MWth	646.4	646.1	648.0
NH_3 flow	tpd	3002.0	3000.4	3047.4
Auxiliaries				
ASU	MWel	62.2	22.1	46.8
Gasifier aux.	MWel	4.1	3.2	3.4
Air/N_2 compression	MWel	0.0	42.7	11.5
Syngas treating	MWel	25.0	3.5	0.6
H_2O pumps	MWel	4.4	2.8	1.4
Heat rejection	MWel	2.3	3.2	1.8
CO_2 compression	MWel	25.6	39.9	2.6
Syngas compression	MWel	30.3	34.1	35.7
Fuel compressor	MWel	0.0	15.5	0.0
Refrigeration	MWel	10.2	11.8	10.2
Total	MWel	164.1	178.7	113.9
Power generation				
Steam turbine	MWel	159.2	93.9	86.3
Gas turbine	MWel	0.0	82.1	0.0
NH_3 turbine	MWel	1.4	1.3	1.4
Energy performance				
η_{NH_3}	%	50.91	53.95	62.25
$\eta_{NH_3,eq}$	%	50.61	53.81	58.99
$\eta_{El.}$	%	−0.27	−0.12	−2.52
SC	GJ/ton	36.5	34.5	29.5
SC_{eq}	GJ/ton	36.8	34.6	31.5
Specific emissions				
E_{CO_2}	kg/ton	−546.2	−552.2	−656.0
C_{CO_2}	kg/ton	3292.4	3186.6	2916.2

consumption required for air enrichment relative to a full ASU is offset by the booster air compressor and additional fuel compressor duties. The MHI concept introduces excess N_2 into the cycle as is required for NH_3 synthesis, the balance of which is removed in the cryogenic purification unit and re-compressed for feeding the gas turbine, elevating overall compression power demand. The MHI plant also requires more CO_2 compression duty than the GE benchmark due to the lower CO_2 delivery pressure from the MDEA unit relative to Selexol, although this is offset by the internal power consumption of the Selexol syngas treating unit. On the other hand, the power generation of the E-gas concept is only about half that of the other concepts, leading to a net negative electrical efficiency, whereas in the GE and MHI concepts generate enough electricity in the steam cycle (and gas turbine for MHI) to be practically self-sufficient. Relative to a natural gas fed NH_3 production plant (KBR) with CCS [6], the GE case shows 8.3 GJ/ton (+29.0%) higher equivalent specific energy consumption, compared to the 6.1 GJ/ton (+21.3%) for the MHI case, while the E-gas concept only 3.0 GJ/ton (+10.7%) higher equivalent energy consumption. The thermal conversion efficiency of fossil fuel to NH_3 is 14.5, 11.5 and 3.2% lower for GE, MHI and E-gas solid-based plants, respectively, relative to natural the gas plant.

In terms environmental performance, complete CO_2 capture is attained in the E-gas advanced oxy-combustion scheme leading to the largest negative emissions. CO_2 emissions originate in GE and MHI concepts from combustion of the PSA off-gas and the cryogenic purifier fuel, respectively, while the MHI case brings additional emissions from the lock hoppers. The specific capture is related to thermal and CO_2 capture performance, achieving the lowest value for the E-gas configuration where a high NH_3 production efficiency outweighs a high CO_2 capture ratio. Co-gasification of biomass and CCS enable a lower environmental impact resulting from negative emissions compared to plants using natural gas as primary energy feedstock. For perspective, an unabated KBR plant emits 1619.5 kg of CO_2 per ton of NH_3. When implementing CCS in the KBR plant, this amount reduces to 278.8 kg/ton [6]. Relative to the latter, the GE, MHI and E-gas cases from solid fuels present 825.0, 830.9, 934.8 kg/ton lower specific CO_2 emissions, respectively.

3.2. Economic results

This section provides a simplified outline of the detailed economic assessments in the SEA tool files available online [49]. Fig. 3 shows that the applied methodology results in attractive cost reductions for the E-gas concept. Relative to the GE and MHI configurations, a 16.6% and 22.4% specific cost decrease is attained, respectively. This saving originates from four main sources. First, the high process efficiency lowers the amount of fuel that must be gasified and treated to produce the required NH_3 output, reducing the size of several costly units. Second, the inherent CO_2 capture achieved by the MAWGS reactor and the subsequent off-gas oxycombustor avoids dedicated CO_2 capture equipment and minimizes CO_2 compressor requirements, although the added cost of the membranes partially offsets this advantage. Third, the inherent purification of hydrogen in the MAWGS reactor avoids the need for a PSA. Fourth, the reduced power generation results in a relatively lower cost for this section. On the other hand, the MHI plant presents the highest capital cost due to the larger gasifier cost (partly due to a higher specific cost of the dry-feed gasifier) that outweighs the scope reduction of the air separation unit. In addition, the larger volumetric flow of the air-blown gasification increases the size of the downstream units. Regarding the synthesis loop, the E-gas and MHI concepts present higher specific costs due to the larger and costlier compression train for syngas generated at approximately 20 bar, whereas the GE configuration produces H_2 at 65 bar, and the N_2 compressor to reach that pressure requires comparatively cheaper carbon steel materials of construction. In the E-gas plant, the estimated membrane surface was 5184 m^2, with a BEC contribution of 6.22 k€/tpd.

The breakdown of specific operational costs for each of the plants is provided in Fig. 4, illustrating the benefit of a CO_2 credit for negative emissions which, under the prices assumed in Table 1, exceeds the cost of the biomass fuel. This advantage is to an extent offset by the higher specific energy price and the cost of CO_2 transport and storage infrastructure. Overall, the E-gas scheme presents 15.4% lower specific operational costs relative to the GE configuration, while minor differences result between the latter and the MHI plant. The E-gas plant achieves lower fuel costs from its higher efficiency, a larger CO_2 credit from near-complete CO_2 capture, and lower FOM due to its lower specific capital costs, although these gains are partially offset by higher VOM resulting from higher electricity consumption and additional membrane replacement costs.

These capital and operating costs are combined into the levelized cost of ammonia (LCOA) presented in Fig. 5. Overall, the E-gas concept results in a 59.0 €/ton (−15.1%) cost decrease with respect to the GE configuration, whereas the MHI configuration presents 18.6 €/ton (4.8%) higher cost. Notably, the cost of product is driven primarily by the capital investment, representing between 45.6 and 48.6% of the total, while the fuel contribution ranges from 27.6 to 30.6% of the levelized cost. Given the large condensation enthalpy of the permeate stream of the E-gas design, a case including revenues for hot water district heating (DH) is included based on the assumptions made in prior work [50], revealing a cost reduction potential of 42.2 €/ton (−12.7%) relative to the original case. For perspective, relative to the KBR process fed with natural gas integrating CCS with an LCOA of 385.9 €/ton [6], the GE and MHI NH_3 plants from solid fuels are 1.5% and 6.3% costlier respectively, while the E-gas concept presents 13.6% lower cost of production.

3.3. Sensitivity assessment

The results of the sensitivity study are presented in Fig. 6. Overall, the three plants behave similarly to changes in the selected parameters, and the cost ranking of the three plants remains unchanged across the entire sensitivity range. Due to large contribution of capital costs to the

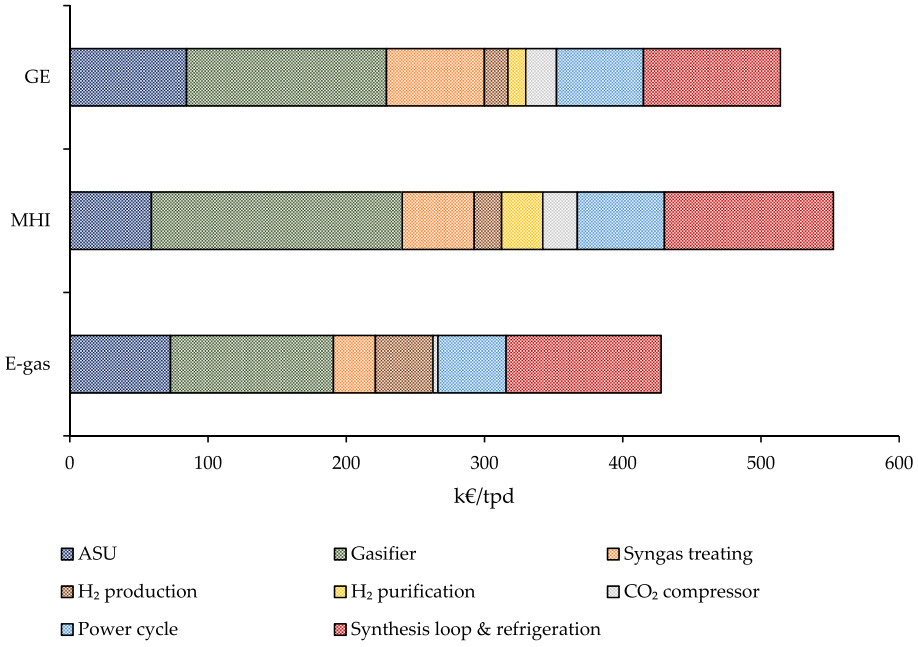

Fig. 3. Specific TOC for the different NH_3 plant configurations.

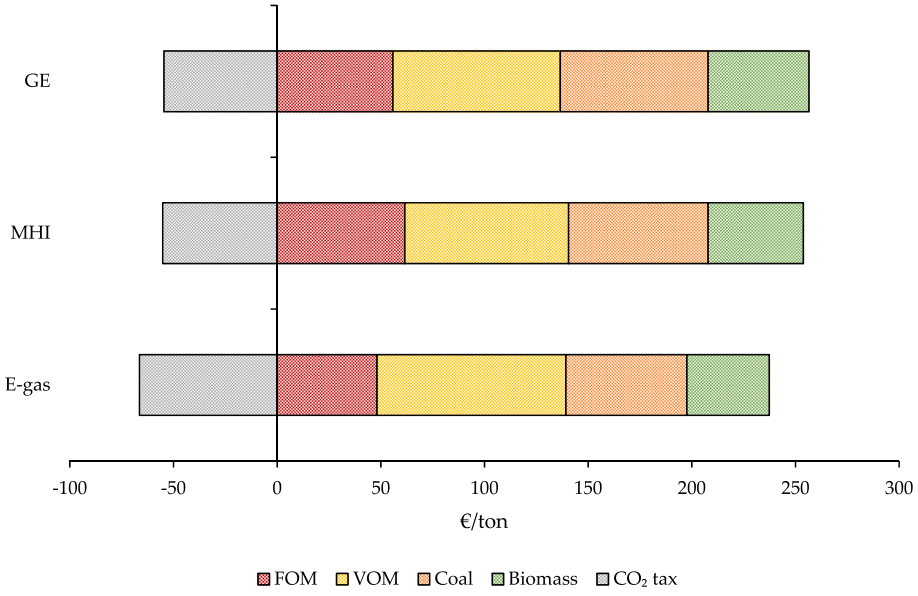

Fig. 4. Specific operational costs for the different NH_3 plants.

LCOA (Fig. 5), the discount rate has the largest influence over the selected sensitivity ranges, illustrating the importance of risk mitigation to secure favourable financing terms. For illustration, the LCOA increases by approximately 5.0% per %-point increase of the discount rate for the MHI configuration, whereas the less capital-intensive natural gas-based counterpart (KBR) evaluated in a prior study [6] almost halves this sensitivity to 2.7% per %-point. Analogously, for the MHI plant the relative LCOA cost increase is 0.74% per %-point decrease in plant capacity factor, while for the KBR concept this relative increase is limited to 0.40% per %-point decrease, highlighting that the disadvantage of increased idle capital is more pronounced in solid fuel plants.

Whereas coal prices are relatively stable, a wider relative range is evaluated for biomass fuel due to the comparatively larger uncertainty. However, the relatively low fraction of biomass heating value in the blended fuel results in similar changes to the LCOA over the selected ranges. Aside from biomass supply costs, pre-processing for better gasification may also influence the biomass price. The E-gas configuration presents the lowest sensitivity due to its high efficiency. Sensitivities to CO_2 pricing and transport & storage are of a similar magnitude to those related to fuel prices. The E-gas concept is the most sensitive to the CO_2 tax due to its high CO_2 capture ratio, but the lower CO_2 production resulting from its high efficiency makes it similarly sensitive to CO_2 T&S costs as the other plants.

Cost assumptions regarding the primary technological uncertainty of the E-gas concept, the membranes in the MAWGS reactor, have only a minor impact, indicating that high costs can be incurred to ensure good membrane performance without compromising the economic viability of the concept. Gasifier costs are a key uncertainty in all plants, imposing an uncertainty comparable to coal pricing on the LCOA. The higher gasifier costs of the dry-fed MHI gasifier makes this plant more sensitive

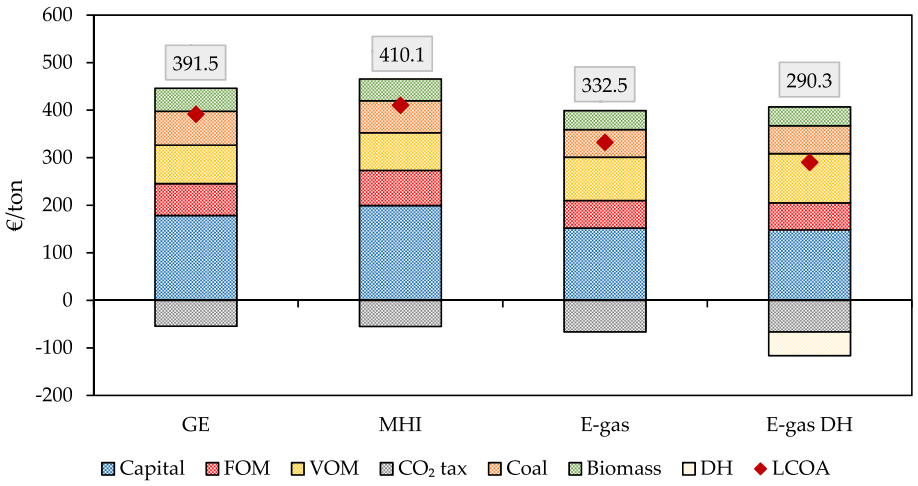

Fig. 5. LCOA of the different NH_3 plants.

than the slurry-fed E-gas and GE plants.

3.4. Benchmarking against relevant alternatives

The technologies assessed in the present work promise a secure supply of decarbonized fuel from local resources at a reasonable cost. To better assess the value offered by these technologies, a consistent comparison to alternative NH_3 supply options is required next to a benchmark representing the current use of unabated fossil fuels. The comparison is conducted from the long-term (mid-century) perspective of Europe as an importing region with the possibility to securely produce more expensive fuels locally or import potentially cheaper fuels from natural gas exporting regions (e.g., the Middle East) assumed to have access to natural gas a low cost of 3 €/GJ. Six cases are compared:

1. E-gas: The innovative E-gas configuration producing NH_3 using locally sourced solid fuels.
2. MHI: The MHI configuration as a more conservative benchmark in case the innovations assumed in the E-gas configuration prove infeasible.
3. GSR-e: Imports of blue NH_3 produced by the innovative GSR technology [6] in natural gas exporting regions (including NH_3 import costs).
4. GSR-i: Local production of blue NH_3 with the GSR technology running on LNG from the same exporting region as in point 3 above (including natural gas liquefaction and import costs).
5. Green: Local production of green NH_3 from the local region with the best wind and solar resources (assumed to be Southern Spain in this European example). This assessment uses wind, solar, and electrolyzer costs projected to the year 2050 [6].
6. LNG: The current solution of consuming LNG directly instead of first converting it to NH_3 (including the CO_2 taxes levied on the unabated use of natural gas).

A reliable comparison to blue NH_3 from natural gas and green NH_3 from renewables is ensured by referring to a previous work by the authors [6] using the same methodology as the present study. LNG assessments are based on other studies (detailed below), which introduce some inconsistencies, but the capital costs of LNG are relatively small next to fuel and emissions costs, so any inconsistencies in this assessment will only have a minor impact on the comparison.

The LNG value chain consists of gas processing, liquefaction and storage, transportation and regasification at the import terminal. Each node contributes both in terms of cost and CO_2 emissions (which is ultimately reflected in the CO_2 tax item) to the final product delivered to the customer. In the case of case 6 above (direct consumption of LNG), end use emissions are also lumped in the estimation. Additional by-product revenues (LPG, condensate etc.) are not considered here for simplicity, but can have a significant impact on project economics. LNG plant and storage capital cost was derived from Raj et al. [51], while the shipping costs were estimated from work of the same group [52]. Based on Katebah et al. [53], CO_2 emissions taking place across the whole LNG value chain were set to 14.3% of the carbon atoms in the primary energy feed. These emissions are assumed to take place prior to delivery at the import terminal.

The system boundary for emissions accounting (used to calculate CO_2 taxes) is drawn at the delivery of fuel to the respective value chains, i.e., upstream emissions related to biomass, coal, natural gas, and renewable electricity production are ignored. Upstream emissions can vary greatly depending on complex and highly case-specific factors such as land-use change for biomass, methane leakages for coal and natural gas, and the carbon-intensity of energy inputs to renewable energy value chains. Detailed accounting of the full lifecycle emissions is therefore beyond the scope of the present study. However, the effect of this simplification should be minor because the upstream emissions of different fuels should be of a similar magnitude and relatively small next to CO_2 produced in the use-phase, especially considering that tighter greenhouse gas regulation will also incentivise measures to reduce upstream emissions.

Fig. 7 reveals the levelized cost of energy determined at the import location for the six cases outlined earlier. NH_3 from E-gas and MHI plants present higher costs than NH_3 from natural gas-based GSR located in an exporting region by 5.2 (41.2%) and 9.4 (74.1%) €/GJ, respectively. If the E-gas plant is positioned in a location where it can supply additional district heating services, this premium reduces to 2.9 €/GJ (23.2%). However, prices of imported fuels are generally considerably higher than the production costs of low-cost exporters because prices are set by the most expensive producer. Furthermore, imported fuel prices can exhibit great volatility following global market disruptions (e.g., the Covid pandemic and Russia-Ukraine war). In this light, the modest price of energy security offered by the local solid fuel plants appears quite reasonable, especially considering the longer-term prospects of the E-gas plant. Achieving energy security via green ammonia is more expensive (71.2% above the E-gas case), and deployment in regions with poorer renewable energy resources than Southern Spain will see considerably higher costs (e.g., 41.5 €/GJ for Northern Germany [6]).

Even though ammonia cannot act as a direct substitute for natural gas in most existing engines and industries, the development of various end-use technologies running on ammonia is feasible within the longer-term view (mid-century) taken by this assessment. Within this context of deploying ammonia as an energy carrier to replace natural gas, Fig. 7 shows that consuming imported NH_3 (GSR-e) is cheaper than consuming

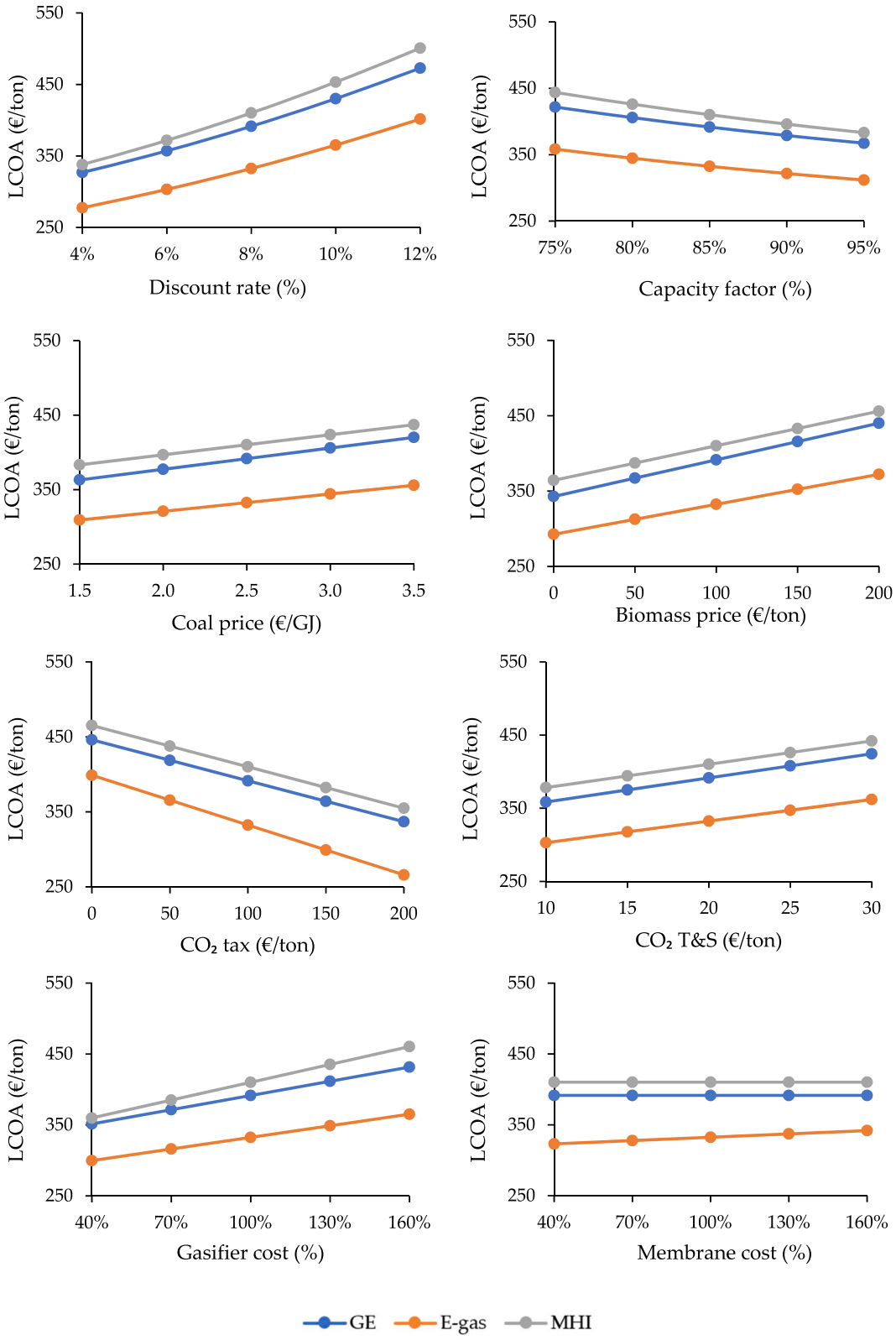

Fig. 6. Sensitivity analysis of the LCOA to different economic assumptions.

imported LNG under the default CO_2 tax of 100 €/ton. The breakeven CO_2 price in this comparison is 60.9 €/ton. A higher CO_2 tax of 127.0 €/ton is required for NH_3 from the E-gas plant to outcompete imported LNG, but the aforementioned price premium and volatility linked to energy imports may justify this higher CO_2 avoidance cost. Fig. 7 also shows that producing ammonia locally from imported natural gas (GSR-i) is much less attractive (50.8% costlier) than importing ammonia produced at the export location (GSR-e). Since international shipping costs are similar between LNG and ammonia, it makes sense to perform only one processing operation on the produced natural gas by

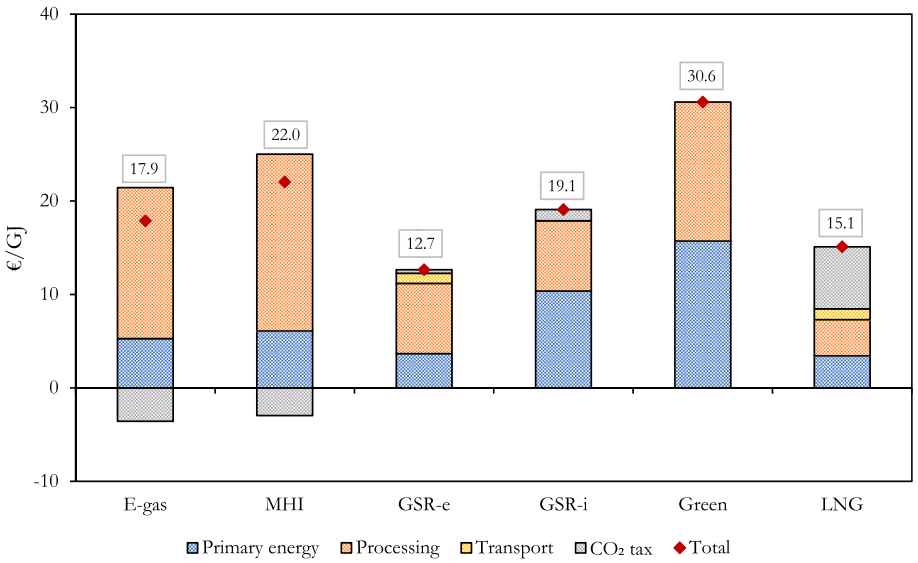

Fig. 7. Benchmarking of NH_3 vs. LNG as energy carriers. Two NH_3 plants from solid fuels (E-gas, MHI), a natural gas based NH_3 process located in exporting and importing regions (GSR-e, GSR-i), and a renewable powered NH_3 route located in Spain (Green) are considered. (For interpretation of the references to colour in this figure legend, the reader is referred to the Web version of this article.)

converting it directly to ammonia close to the production well.

3.5. Policy recommendations

Currently, the decarbonization strategies of energy importing regions like Europe rely heavily on renewables (largely wind and solar). However, this strategy faces several challenges such as the cost and complexity of integrating high shares of intermittent generators, public resistance to onshore wind and transmission expansions, rising cost, supply security and environmental concerns related to critical minerals [54], and complex value chains with an overdependence on China [55]. Furthermore, electricity currently supplies only 25% of final energy in Europe (20% globally) [56], requiring tremendous electrification efforts in a renewables-led decarbonization effort.

The availability of affordable, locally produced, negative-emission fuels would address all these challenges. At 17.9 €/GJ (64.4 €/MWh), Fig. 8 shows that NH_3 from the carbon-negative E-gas concept would be cost competitive with current unabated NH_3 supply, which accounts for 1.3% of global emissions [57]. Furthermore, Europe has centuries of remaining coal resources [56], and the biomass blend ratio can be adjusted to maximize negative emissions within the bounds of sustainable biomass supply. Due to the ease of transporting and storing ammonia in liquid form, plants can be constructed close to CO_2 storage reservoirs to avoid problems with access to CO_2 transport and storage infrastructure.

For these reasons, policy incentives supporting the expansion of locally produced, low-carbon fuels are recommended in energy importing regions such as Europe. Action is needed both on the supply and demand sides. Supply-side incentives should be technology neutral with equal support for green and blue solutions, letting the market determine the optimal technology mix. Energy security can be encouraged by making incentives proportional to the fraction of the overall technology value chain sourced from local markets. In parallel, demand-side incentives are needed to overcome the chicken-and-egg problem facing low-carbon fuels such as ammonia that currently lack reliable demand in the energy sector. This combination of support for local fuel production and guaranteed demand for the produced fuel will mobilize the investment required to establish complete value chains and develop advanced solutions like the E-gas concept proposed in this study.

4. Summary & conclusions

In this work, a techno-economic assessment of three process configurations for ammonia production from coal blended with 30%w biomass was carried out, employing different entrained flow gasification technologies: two slurry-fed oxygen blown systems (GE & E-gas) and a

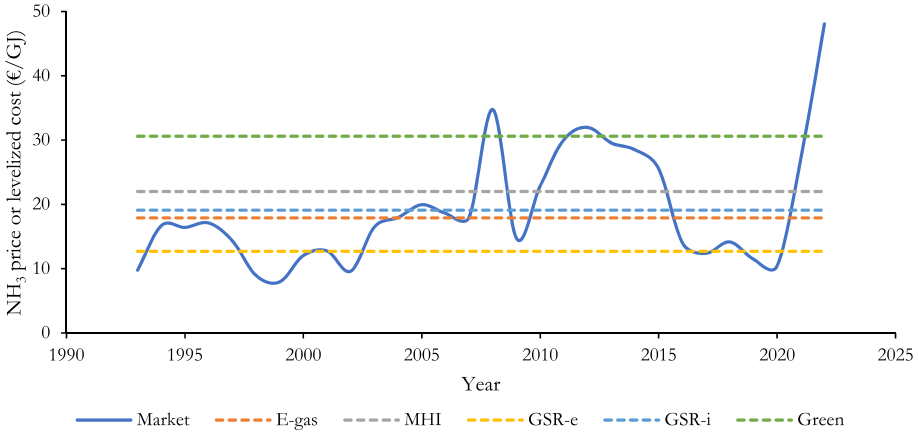

Fig. 8. Inflation-adjusted historical NH_3 prices [58] against production costs for different avenues.

dry-fed air blown technology (MHI). The GE plant utilizes Selexol absorption and a PSA unit for H_2 production, while the MHI configuration employs a cryogenic purification unit to supply syngas to the loop. Finally, the advanced E-gas plant features feed slurry vaporization and a membrane reactor to maximize fuel conversion efficiency to H_2 with inherent carbon capture of the retentate stream. The three plants illustrate different approaches to process design: GE is the reference technology, MHI offers an example of transposition of de-risked commercial process units constituting an innovative design, while the E-gas configuration illustrates the potential of step-change technologies currently under development. The main results of the study are outlined below:

- From an energy perspective, the GE plant reached an equivalent specific energy consumption (SC_{eq}) of 36.8 GJ/ton. Largely due to more efficient gasification, the E-gas counterpart reduced SC_{eq} by 5.2 GJ/ton (−14.2%) and the MHI design by 2.2 GJ/ton (−6.3%).
- Biomass blending allowed negative CO_2 emissions in all cases: 546.2 $kgCO_2$/ton for GE, −552.2 $kgCO_2$/ton for MHI, and −656.0 kg/ton for E-gas. The improved emissions performance of the E-gas concept results from the complete CO_2 capture inherent in the process design that produces no flue gas (and thus no air pollutants). This concept also produced the least CO_2 per unit of product due to its high efficiency.
- The GE configuration attains a levelized cost of ammonia (LCOA) of 391.5 €/ton. In comparison, the E-gas plant presents a reduction of 59.0 €/ton (15.1%), resulting from decreased capital and fuels costs, while the MHI concept yields a cost increase of 18.6 €/ton (4.8%), primarily due to the larger gasifier capital expenditure. Exports of 120 °C water for district heating can reduce the LCOA of the E-gas concept by a further 12.7%. The discount rate was the most influential economic parameter in the assessment due to the high capital intensity of solid-fuel processing plants (representing between 45.5 and 48.6% of the LCOA).
- Benchmarking against alternative NH_3 supply pathways by mid-century revealed that energy security from local solid fuels comes at a 5.2 €/GJ premium relative to imports from natural gas producing regions. Green NH_3 supply in regions with excellent solar resources costs 12.7 €/GJ more than the solid fuel alternative.

The primary conclusion from this work is that continued technological development can unlock significant, albeit not game-changing, cost reductions in ammonia production from solid fuels, and that the resulting carbon-negative fuel offers cost-effective energy security to energy importers in a low-carbon future. Although ammonia production in natural gas exporting regions can be cheaper, it is likely that market prices of such imported fuel will be considerably higher and more volatile, justifying investments in plants to produce ammonia from locally available solid fuels. For this reason, technology-neutral policy support for locally produced fuels is recommended in energy importing regions. Such incentives will naturally drive the investments required for advances such as the E-gas process configuration proposed in this work.

Finally, it must be highlighted that a transition to ammonia (or hydrogen) as an energy carrier will require large parallel investments in the development and deployment of new distribution and end-use infrastructure. Policy support will be required to address this chicken-and-egg problem via coordinated incentives to expand supply and demand concurrently. Furthermore, CO_2 pricing may remain at low levels in developing world regions where economic upliftment remains the foremost priority, preserving the competitiveness of carbonaceous fuels such as LNG or gasoline. Thus, carbon-free fuels like ammonia do not present a silver bullet for global decarbonization, although they are becoming viable in wealthier economies with high CO_2 taxes. Continued growth will be region-specific and will require careful consideration of energy affordability, security, and practical usability.

Credit author statement

Carlos Arnaiz del Pozo: Conceptualization, Methodology, Formal analysis, Investigation, Writing – original draft, Visualization Schalk Cloete: Conceptualization, Methodology, Formal analysis, Writing – original draft, Writing – review & editing Ángel Jiménez Álvaro: Writing – review & editing, Supervision, Funding acquisition

Declaration of competing interest

The authors declare that they have no known competing financial interests or personal relationships that could have appeared to influence the work reported in this paper.

Data availability

The manuscript contains a link to a SharePoint folder containing the full economic assessment sheets.

Acknowledgements

The authors would like to acknowledge Honeywell for the free academic license of Unisim Design R481. The authors would like to acknowledge AmsterCHEM for the free academic CAPE-OPEN license. This research received funding from the European Union NextGenerationEU, Ministerio de Universidades grant RD 289/2021.

Appendix A. Supplementary data

Supplementary data to this article can be found online at https://doi.org/10.1016/j.energy.2023.127880.

References

[1] Intergovernmental Panel on Climate Change, (IPCC). Climate change 2022 mitigation of climate change. 2022.
[2] IEA. Global hydrogen review 2021. Paris: International Energy Agency; 2021.
[3] Nazir H, Muthuswamy N, Louis C, Jose S, Prakash J, Buan ME, Flox C, Chavan S, Shi X, Kauranen P. Is the H2 economy realizable in the foreseeable future? Part II: H2 storage, transportation, and distribution. Int J Hydrogen Energy 2020;45(41): 20693–708.
[4] IEA. The Future of Hydrogen, IEA, Paris. 2019. https://www.iea.org/reports/the-future-of-hydrogen.
[5] Alguacil FJ, Robla JI. Innovative processes in the production of inorganic bases and derived salts of current interest. Physical Sciences Reviews 2020;5:8.
[6] Arnaiz del Pozo C, Cloete S. Techno-economic assessment of blue and green ammonia as energy carriers in a low-carbon future. Energy Convers Manag 2022; 255:115312.
[7] Pattabathula V, Richardson J. Introduction to ammonia production. CEP Magazine 2016;2:69–75.
[8] Heffer P, Prud'homme M. Global nitrogen fertilizer demand and supply: trend, current level and outlook. 2016.
[9] Yapicioglu A, Dincer I. A review on clean ammonia as a potential fuel for power generators. Renewable and Sustainable Energy Reviews 2019;103:96–108.
[10] Ghavam S, Vahdati M, Wilson IAG, Styring P. Sustainable ammonia production processes. Front Energy Res 2021;9.
[11] Arora P, Sharma I, Hoadley A, Mahajani S, Ganesh A. Remote, small-scale, 'greener' routes of ammonia production. J Clean Prod 2018;199:177–92.
[12] Higman C. Gasification. second ed. 2008.
[13] Hannemann F, Schiffers U, Karg J, Kanaar M. V94. 2 Buggenum experience and improved concepts for syngas applications 2002:27–30.
[14] Thallam Thattai A, Oldenbroek V, Schoenmakers L, Woudstra T, Aravind PV. Experimental model validation and thermodynamic assessment on high percentage (up to 70%) biomass co-gasification at the 253MWe integrated gasification combined cycle power plant in Buggenum, The Netherlands. Appl Energy 2016; 168:381–93.
[15] Habgood DCC, Hoadley AFA, Zhang L. Techno-economic analysis of gasification routes for ammonia production from Victorian brown coal. Chem Eng Res Des 2015;102:57–68.
[16] Toporov D, Abraham R. Gasification of low-rank coal in the High-Temperature Winkler (HTW) process. J S Afr Inst Min Metall 2015;115(7):589–97.
[17] Xu J, Yang Y, Li Y. Recent development in converting coal to clean fuels in China. Fuel 2015;152:122–30.
[18] Zoelle AJ, Turner MJ, Woods MC, , James III PhD, Robert E, Fout TE, Shultz TR. In: "Cost and performance baseline for fossil energy plants, volume 1: bituminous coal and natural gas to electricity, revision 4" *Cost and performance Baseline for fossil*

energy plants. ume 1. Bituminous Coal and Natural Gas to Electricity; 2018. *Revision*.
[19] Flórez-Orrego D, de Oliveira Junior S. Modeling and optimization of an industrial ammonia synthesis unit: an exergy approach. Energy 2017;137:234–50.
[20] Ieaghg L Mancuso, Ferrari N, Davison J. Capture at coal based power and hydrogen plants. IEAGHG Report 2014/3 2014.
[21] Gräbner M, Meyer B. Performance and exergy analysis of the current developments in coal gasification technology. Fuel 2014;116:910–20.
[22] Giuffrida A, Romano M, Lozza G. Thermodynamic assessment of IGCC plants with hot gas desulphurization. Appl Energy 2010;87(11):3374–83.
[23] Amelio M, Morrone P, Gallucci F, Basile A. Integrated gasification gas combined cycle plant with membrane reactors: technological and economical analysis. Energy Convers Manag 2007;48(10):2680–93.
[24] Jordal K, Anantharaman R, Peters TA, Berstad D, Morud J, Nekså P, Bredesen R. High-purity H2 production with CO2 capture based on coal gasification. Energy 2015;88:9–17.
[25] Zhang K. 5 - recent progress on sulfur-resistant palladium membranes. 2020. p. 123–37.
[26] Wassie SA, Medrano JA, Zaabout A, Cloete S, Melendez J, Tanaka DAP, Amini S, van Sint Annaland M, Gallucci F. Hydrogen production with integrated CO2 capture in a membrane assisted gas switching reforming reactor: proof-of-Concept. Int J Hydrogen Energy 2018;43(12):6177–90.
[27] Dyson DC, Simon JM. Kinetic expression with diffusion correction for ammonia synthesis on industrial catalyst. Ind Eng Chem Fund 1968;7(4):605–10.
[28] Anantharaman R, Bolland O, Booth N, Van Dorst E, Sanchez Fernandez E, Franco F, Macchi E, Manzolini G, Nikolic D, Pfeffer A, Prins M, Rezvani S, Robinson L. Cesar deliverable D2.4.3. European Best Practice Guidelines For Assessment Of Co2 Capture Technologies; 2018.
[29] Qin K, Lin W, Jensen PA, Jensen AD. High-temperature entrained flow gasification of biomass. Fuel 2012;93:589–600.
[30] Honeywell. Unisim thermo reference guide R480 release. 2020.
[31] Kapetaki Z, Brandani S, Brandani P, Ahn H. Process simulation of a dual-stage Selexol process for 95% carbon capture efficiency at an integrated gasification combined cycle power plant. Int J Greenh Gas Control 2015;39:17–26.
[32] Nazir SM, Cloete JH, Cloete S, Amini S. Efficient hydrogen production with CO2 capture using gas switching reforming. Energy 2019;185:372–85.
[33] Giuffrida A, Romano MC, Lozza G. Thermodynamic analysis of air-blown gasification for IGCC applications. Appl Energy 2011;88(11):3949–58.
[34] Giuffrida A, Romano MC, Lozza G. Efficiency enhancement in IGCC power plants with air-blown gasification and hot gas clean-up. Energy 2013;53:221–9.
[35] Hashimoto T, Sakamoto K, Kitagawa Y, Hyakutake Y, Setani N. Development of IGCC commercial plant with air-blown gasifier. Mitsubishi Heavy Industries Technical Review 2009;46(2):1–5.
[36] Guo X, Vanhaecke E, Vullum PE, Ma J, Gunawardana PDS, Walmsley JC, Chen D, Venvik HJ. Effects of metal dusting relevant exposures of alloy 601 surfaces on carbon formation and oxide development. Catal Today 2021;369:48–61.
[37] Moioli S, Giuffrida A, Romano MC, Pellegrini LA, Lozza G. Assessment of MDEA absorption process for sequential H2S removal and CO2 capture in air-blown IGCC plants. Appl Energy 2016;183:1452–70.
[38] Bonalumi D, Giuffrida A. Investigations of an air-blown integrated gasification combined cycle fired with high-sulphur coal with post-combustion carbon capture by aqueous ammonia. Energy 2016;117:439–49.
[39] G.H. Badeer, "GE aeroderivative gas turbines - design and operating features" *GE power systems*. Evendale, OH..
[40] Mansouri Majoumerd M, Raas H, De S, Assadi M. Estimation of performance variation of future generation IGCC with coal quality and gasification process – simulation results of EU H2-IGCC project. Appl Energy 2014;113:452–62.
[41] Arnaiz del Pozo C, Cloete S, Jiménez Álvaro Á. Carbon-negative hydrogen: exploring the techno-economic potential of biomass co-gasification with CO2 capture. Energy Convers Manag 2021;247:114712.
[42] Fernandez E, Medrano JA, Melendez J, Parco M, Viviente JL, van Sint Annaland M, Gallucci F, Pacheco Tanaka DA. Preparation and characterization of metallic supported thin Pd–Ag membranes for hydrogen separation. Chem Eng J 2016;305:182–90.
[43] Hla SS, Park D, Duffy GJ, Edwards JH, Roberts DG, Ilyushechkin A, Morpeth LD, Nguyen T. Kinetics of high-temperature water-gas shift reaction over two iron-based commercial catalysts using simulated coal-derived syngases. Chem Eng J 2009;146(1):148–54.
[44] Abad A, Adánez J, García-Labiano F, de L, Diego F, Gayán P, Celaya J. Mapping of the range of operational conditions for Cu-, Fe-, and Ni-based oxygen carriers in chemical-looping combustion. Chem Eng Sci 2007;62(1–2):533–49.
[45] Arnaiz del Pozo Carlos, Cloete Schalk, Ángel Jiménez Álvaro. Standard economic assessment (SEA) tool. https://bit.ly/3hyF1TT.
[46] Arnaiz del Pozo Carlos, Cloete Schalk, Ángel Jiménez Álvaro. SEA tool user guide. https://bit.ly/3jq9Bkf.
[47] Turton R, Bailie RC, Whiting WB, Shaeiwitz JA. Analysis, synthesis and design of chemical processes. 2008.
[48] R.2. DOE/NETL-2010/1397. Cost performance baseline for fossil energy plants. Volume 1: bituminous coal and natural gas to electricity. In: performance baseline for fossil energy plants. ume 1. Bituminous coal and natural gas to electricity; 2013.
[49] Arnaiz del Pozo C, Cloete S, Á Jiménez Álvaro. Ammonia from solid fuels. SEA tool files. 2022. https://bit.ly/3dXWI03.
[50] Arnaiz del Pozo C, Cloete S, Jiménez Álvaro Á. Carbon-negative hydrogen: exploring the techno-economic potential of biomass co-gasification with CO2 capture. Energy Convers Manag 2021;247:114712.
[51] Raj R, Suman R, Ghandehariun S, Kumar A, Tiwari MK. A techno-economic assessment of the liquefied natural gas (LNG) production facilities in Western Canada. Sustain Energy Technol Assessments 2016;18:140–52.
[52] Raj R, Ghandehariun S, Kumar A, Geng J, Linwei M. "A techno-economic study of shipping LNG to the Asia-Pacific from Western Canada by LNG carrier". J Nat Gas Sci Eng 2016;34:979–92.
[53] Katebah MA, Hussein MM, Shazed A, Bouabidi Z, Al-musleh EI. Rigorous simulation, energy and environmental analysis of an actual baseload LNG supply chain. Comput Chem Eng 2020;141:106993.
[54] International Energy Agency. The role of critical minerals in clean energy transitions. 2021.
[55] International Energy Agency. "Energy Technology Perspectives. 2023. https://www.iea.org/reports/energy-technology.
[56] International Energy Agency. World energy outlook. 2022.
[57] Ammonia technology roadmap, IEA. https://www.iea.org/reports/ammonia-technology-roadmap. License: CC BY 4.0 2021.
[58] https://www.usgs.gov/centers/national-minerals-information-center/nitrogen-statistics-and-information. accessed April 2023.